Gravitino dark matter and neutrino masses in partial split supersymmetry

Marco Aurelio Díaz, Sebastián García Sáenz, and Benjamin Koch

Departamento de Física, Pontificia Universidad Católica de Chile, Avenida Vicuña Mackenna 4860, Santiago, Chile

Partial split supersymmetry with bilinear R-parity violation allows one to reproduce all neutrino mass and mixing parameters. The viable dark matter candidate in this model is the gravitino. We study the hypothesis that both possibilities are true: partial split supersymmetry explains neutrino physics and dark matter is actually composed of gravitinos. Since the gravitino has a small but nonzero decay probability, its decay products could be observed in astrophysical experiments. Combining bounds from astrophysical photon spectra with the bounds coming from the mass matrix in the neutrino sector we derive a stringent upper limit for the allowed gravitino mass. This mass limit is in good agreement with the results of direct dark matter searches.

I. INTRODUCTION

Split supersymmetry (SS) was originally proposed to address some of the most salient problems of supersymmetric models, which are fast proton decay, excessive flavor changing neutral currents, and excessive *CP* violation [1]. In SS the solution to these problems is accomplished by considering all squarks and sleptons very massive, with a mass scale $\tilde{m}$ somewhere between the supersymmetric scale M_{susy} and the grand unification scale M_{GUT}. One of the Higgs bosons remains light, as usual in supersymmetric models, as well as the gauginos and Higgsinos, with all these particles having a mass accessible to the LHC [2].

If R-parity violation (RPV) is introduced in supersymmetric models, lepton number and/or baryon number will be violated as well, inducing a potentially too-fast proton decay [3]. Nevertheless, in SS the trilinear RPV couplings play little role in the phenomenology, with the exception being in the gluino decay rate. In this case, only bilinear RPV (BRPV) is relevant, opening up the possibility for a neutrino mass generation mechanism, without running into the danger of a too-fast proton decay. As in any BRPV model, in SS-BRPV the atmospheric neutrino mass squared difference is generated by a low-energy seesaw mechanism due to the mixing between neutrinos and neutralinos [4,5]. Nevertheless, at one loop the only contributions to the neutrino mass matrix, coming from loops with the Higgs boson and neutralinos, is not enough to generate a solar neutrino mass squared difference [6,7]. Thus, an additional contribution to the model is needed [8] or the model itself has to be generalized.

In partial split supersymmetry (PSS) all squarks and sleptons have a mass of the order of the SS mass scale $\tilde{m}$, but both Higgs doublets remain with a mass at the electroweak scale [7,9]. The addition of RPV to this model was introduced to be able to generate a solar neutrino mass [7]. Loop contributions from neutral *CP*-even and *CP*-odd Higgs bosons are indeed able to do the job, producing not only the atmospheric and solar masses, but also the atmospheric, solar, and reactor neutrino mixing angles [10].

Because R-parity is not conserved, the lightest supersymmetric particle (LSP) will be unstable and decay into standard-model particles. This will occur very fast if the LSP is the traditional neutralino, losing it as a candidate for dark matter. It is however known that in the case of a gravitino LSP, despite being unstable, it will decay very slowly via gravitationally induced couplings [11,12]. Suppression of the gravitino interactions by both the Planck mass and the R-parity violating couplings leads to a very long-lived massive particle, whose lifetime can typically be of several orders of magnitude longer than the age of the Universe. The next-to-lightest superparticle (NLSP), on the other hand, has a lifetime which is much shorter than 1 s, and thus becomes harmless to a successful big-bang nucleosynthesis [13].

The fact that the gravitino decays to ordinary particles in such a scenario has given rise to interesting phenomenological studies [14–16]. An important one is the study of the photon spectrum produced from the two-body decay [17–19], and more recently from the three-body decays of the gravitino [20,21]. Important constraints on the mass and lifetime of the gravitino can be derived from the fact that its decay has not been detected by gamma-ray telescopes, most importantly the Fermi Large Area Telescope (Fermi LAT) [22–26].

Further constraints on the allowed parameters can be derived from the measurements of the neutrino masses and mixing parameters, which in PSS provide constraints on the R-parity violating couplings [7,10].

In this work we study these two independent constraints, and show that when taken together they imply the existence of a maximal value of the light gravitino mass $m_{3/2}^{\text{max}}$, and also the existence of a minimum value of the gravitino lifetime. Our findings are in good agreement with direct dark matter searches [27,28] which put much stronger constraints on dark matter particles with masses $\gg m_{3/2}^{\text{max}}$.

It is important to mention that this kind of model can be further studied in the context of the observed Pamela electron/positron excess and direct LHC signals [29,30]. Further studies are possible in the context of the early Universe [31–33]. However, since in our work the gravitino has an extremely long lifetime, the implications from gravitino decay in the early Universe are not taken into account.

This model is a bottom-up approach; it can however be motivated by a number of general considerations. In Ref. [34] it is shown that a split supersymmetric spectrum can be easily generated in models with direct mediation of supersymmetry breaking, i.e., without invoking a hidden sector. In opposition to low-energy supersymmetric models, in SS this is possible because the gauginos are allowed to be much lighter than the sfermions. A toy model is given, where sfermion masses are generated at a scale $\tilde{m}$, while gaugino masses are induced at a lower scale μ, after integrating out physics at a higher scale that controls the supersymmetry breaking. In the same model, a gravitino mass is generated at the scale $\tilde{m}^2/M_{\mathrm{Pl}}$, allowing it to be even lighter than gauginos. This toy model generates also a B_μ term of the order of $\tilde{m}^2$ and it would have to be modified in order to accommodate PSS, where B_μ is required to be much smaller than $\tilde{m}^2$. It is worth mentioning that a $B_\mu \ll \tilde{m}^2$ would alleviate the otherwise present fine-tuning needed in the Higgs potential to generate a correct electroweak symmetry breaking [35]. As a top-down approach to PSS we mention also Ref. [9], where a PSS spectrum is given. In this model sfermion masses are generated at a scale $\tilde{m}^2 \sim V_0/M^2$, where supersymmetry breaking originates with a hidden sector dynamics with vacuum energy V_0, and sfermion contributions are communicated to the visible sector by massive fields of mass M. In addition, two light Higgs scalars are composite with a mass $m_h \sim \frac{g}{4\pi}\Lambda_{\mathrm{comp}}$, with Λ_{comp} the typical scale of the strong dynamics. The gravitino mass is of the order $\sqrt{V_0}/M_{\mathrm{Pl}}$ and can be the LSP for values for example $V_0 \sim (10^9 \text{ GeV})^4$.

II. PARTIAL SPLIT SUPERSYMMETRY

In PSS both Higgs doublets remain with a mass at the electroweak scale. As it happens in SS, Higgsinos, gauginos, and Higgs bosons interact via induced couplings of the type

$$\mathcal{L}_{\mathrm{PSS}}^{\mathrm{RPC}} \ni -\frac{1}{\sqrt{2}}H_u^\dagger(\tilde{g}_u\sigma\tilde{W} + \tilde{g}_u'\tilde{B})\tilde{H}_u$$
$$-\frac{1}{\sqrt{2}}H_d^\dagger(\tilde{g}_d\sigma\tilde{W} - \tilde{g}_d'\tilde{B})\tilde{H}_d + \mathrm{H.c.}, \quad (1)$$

where RPC is R-parity conserving and $\tilde{g}_u$, $\tilde{g}_u'$, $\tilde{g}_d$, and $\tilde{g}_d'$ are couplings induced in the effective low-energy Lagrangian. At the SS scale $\tilde{m}$ they satisfy the boundary conditions,

$$\tilde{g}_u = \tilde{g}_d = g, \qquad \tilde{g}_u' = \tilde{g}_d' = g', \quad (2)$$

evolving with independent renormalization group equation down to the electroweak scale. Similarly to the minimal supersymmetric standard model (MSSM), both Higgs fields acquire a vacuum expectation value $\langle H_u \rangle = v_u$ and $\langle H_d \rangle = v_d$, with the constraint $v^2 = v_u^2 + v_d^2 = 246 \text{ GeV}^2$ and the definition $\tan\beta = v_u/v_d$. Gauginos and Higgsinos mix forming the neutralinos, with a mass matrix very similar to the one in the MSSM,

$$M_{\chi^0} = \begin{bmatrix} M_1 & 0 & -\frac{1}{2}\tilde{g}_d'c_\beta v & \frac{1}{2}\tilde{g}_u's_\beta v \\ 0 & M_2 & \frac{1}{2}\tilde{g}_d c_\beta v & -\frac{1}{2}\tilde{g}_u s_\beta v \\ -\frac{1}{2}\tilde{g}_d'c_\beta v & \frac{1}{2}\tilde{g}_d c_\beta v & 0 & -\mu \\ \frac{1}{2}\tilde{g}_u's_\beta v & -\frac{1}{2}\tilde{g}_u s_\beta v & -\mu & 0 \end{bmatrix},$$

$$(3)$$

where M_1 and M_2 are the gaugino masses associated with the $U(1)$ and $SU(2)$ gauge bosons, and μ is the Higgsino mass. In our calculations we will neglect the running of the Higgsino-Higgs-gaugino couplings and work with their approximated value indicated by Eq. (2).

The addition of R-parity violation to the PSS Lagrangian allows us to study a mechanism for neutrino mass generation. Trilinear couplings are not relevant for this problem, because all squarks and sleptons are very heavy, with a mass of the order of $\tilde{m}$, and thus decoupled from the low-energy effective theory. Only BRPV is relevant, and is described by the terms

$$\mathcal{L}_{\mathrm{PSS}}^{\mathrm{RPV}} = -\epsilon_i\tilde{H}_u^T\epsilon L_i - \frac{1}{\sqrt{2}}b_i H_u^T\epsilon(\tilde{g}_d\sigma\tilde{W} - \tilde{g}_d'\tilde{B})L_i + \mathrm{H.c.},$$

$$(4)$$

where $\epsilon = i\sigma_2$. The ϵ_i are the supersymmetric BRPV parameters in the superpotential, which at the low scale manifest themselves as mixing between Higgsinos and lepton fields. The b_i are three dimensionless parameters attached to lepton-Higgs-gaugino interactions. They are analogous to the ones in Eq. (1), except that they violate R-parity and are generated in the effective low-energy theory.

The origin of the BRPV terms in (4) is related to the μ-problem which refers to the origin of the term $\mu H_u H_d$ in the superpotential. As discussed for example in Ref. [36], the same mechanism that solves the μ-problem could be used to explain the origin of the ϵ terms. A popular mechanism is the existence of nonrenormalizable couplings of the sort $(a/M_{\mathrm{Pl}})\Phi_1\Phi_2 H_u H_d$, with a being a dimensional constant and Φ_1 and Φ_2 two hidden sector scalars. When supersymmetry breaks and Φ_1 and Φ_2 acquire vacuum expectation values a μ-term is generated. Similar terms $(a_i/M_{\mathrm{Pl}})\Phi_3\Phi_4 H_u L_i$ can be present generating ϵ-terms, although a_i and/or $\langle\Phi_3\rangle$, $\langle\Phi_4\rangle$ should be much smaller than a and/or $\langle\Phi_1\rangle$, $\langle\Phi_2\rangle$ in order to have ϵ_i a few

order of magnitude smaller than μ, necessary for neutrino physics. The b_i terms are generated after integrating out the sleptons, and appear because above the scale $\tilde{m}$ the Higgs bosons mix with sleptons. At the scale $\tilde{m}$ we have $b_i \sim v_i/v_u$, with the necessary condition $v_u B_{\epsilon i} \sim v_i M_{Li}^2$ from the minimization of the scalar potential [7]. Large $B_{\epsilon i}$ can be easily obtained in a similar way as for B_μ, as explained in [34]. We mention also Ref. [37] where R-parity is naturally broken radiatively when a right-handed sneutrino acquires a vacuum expectation value, generating bilinear R-parity violating terms. In our work, we concentrate on the effect of bilinear R-parity violation. Trilinear R-parity violating couplings could be present, but we ignore their effects due to the large mass of the sfermions.

III. NEUTRINO MASSES

When Higgs bosons acquire vacuum expectation values, mixing terms between gauginos and leptons are generated, producing the following mixing between neutrinos and heavier fermions:

$$\mathcal{L}_{\mathrm{PSS}}^{\mathrm{RPV}} = -\left[\epsilon_i \tilde{H}_u^0 + \frac{1}{2}b_i v_u(\tilde{g}_d \tilde{W}_3 - \tilde{g}_d' \tilde{B})\right]\nu_i + \mathrm{H.c.} + \cdots.$$

(5)

The effect of these terms is that neutralinos mix with neutrinos, forming a 7×7 mass matrix, which in the basis $(\tilde{B}, \tilde{W}, \tilde{H}_u, \tilde{H}_d, \nu_e, \nu_\mu, \nu_\tau)$ has the form

$$\mathcal{M}_N = \begin{bmatrix} M_{\chi^0} & m^T \\ m & 0 \end{bmatrix},$$

(6)

and where the 4×4 submatrix M_{χ^0} is the neutralino mass matrix in Eq. (3). The 4×3 neutralino-neutrino mixing block

$$m = \begin{bmatrix} -\frac{1}{2}\tilde{g}_d' b_1 v_u & \frac{1}{2}\tilde{g}_d b_1 v_u & 0 & \epsilon_1 \\ -\frac{1}{2}\tilde{g}_d' b_2 v_u & \frac{1}{2}\tilde{g}_d b_2 v_u & 0 & \epsilon_2 \\ -\frac{1}{2}\tilde{g}_d' b_3 v_u & \frac{1}{2}\tilde{g}_d b_3 v_u & 0 & \epsilon_3 \end{bmatrix}$$

(7)

develops from terms in Eq. (5). A diagonalization by blocks of the mass matrix in Eq. (6) can be achieved by a rotation $\mathcal{N} \mathcal{M}_N \mathcal{N}^T$, given by

$$\mathcal{N} \simeq \begin{bmatrix} N & N\xi^T \\ -\xi & 1 \end{bmatrix},$$

(8)

where we define

$$\xi = m M_{\chi^0}^{-1},$$

(9)

with

$$\xi_{i1} = \frac{\tilde{g}_d' \mu M_2}{2 \det M_{\chi^0}} \Lambda_i$$

$$\xi_{i2} = -\frac{\tilde{g}_d \mu M_1}{2 \det M_{\chi^0}} \Lambda_i$$

$$\xi_{i3} = \frac{v_u}{4 \det M_{\chi^0}}(M_1 \tilde{g}_u \tilde{g}_d + M_2 \tilde{g}_u' \tilde{g}_d')\Lambda_i - \frac{\epsilon_i}{\mu}$$

$$\xi_{i4} = -\frac{v_d}{4 \det M_{\chi^0}}(M_1 \tilde{g}_d^2 + M_2 \tilde{g}_d'^2)\Lambda_i$$

(10)

and $\Lambda_i = \mu b_i v_u + \epsilon_i v_d$. This leaves an induced effective neutrino mass matrix equal to

$$\mathbf{M}_\nu^{(0)}|_{ij} = -m^T M_{\chi^0}^{-1} m|_{ij} = A^{(0)} \Lambda_i \Lambda_j,$$

(11)

with

$$A^{(0)} = \frac{M_1 \tilde{g}_d^2 + M_2 \tilde{g}_d'^2}{4 \det M_{\chi^0}}.$$

(12)

At this level only one neutrino acquires mass, leaving the solar squared mass difference null and the solar angle undetermined. Quantum corrections contribute to the neutrino mass matrix in such a way that the degeneracy in Eq. (11) is lifted, leaving it with the following form:

$$\mathbf{M}_\nu|_{ij} = A\Lambda_i \Lambda_j + C\epsilon_i \epsilon_j,$$

(13)

where the B-term [10] has been made to vanish by an appropriate choice of the subtraction point. Thus at one loop two neutrinos acquire a mass while the third one remains massless. Since in this case the experimental value $\Delta m_{\mathrm{sol}}^2/\Delta m_{\mathrm{atm}}^2 \approx 0.035$ implies $m_{\nu_3} \gg m_{\nu_2}$, we have

$$\Delta m_{\mathrm{atm}}^2 \approx (A|\vec{\Lambda}|^2 + C|\vec{\epsilon}|^2)^2 - 2AC|\vec{\Lambda} \times \vec{\epsilon}|^2,$$

$$\Delta m_{\mathrm{sol}}^2 \approx \frac{A^2 C^2 |\vec{\Lambda} \times \vec{\epsilon}|^4}{(A|\vec{\Lambda}|^2 + C|\vec{\epsilon}|^2)^2}.$$

(14)

For later use, we introduce the photino $\tilde{\gamma}$ and zino $\tilde{Z}$ fields by rotating by the weak mixing angle the weakly interacting gauginos $\tilde{B}$, $\tilde{W}$, in direct analogy to their standard model counterparts,

$$\begin{pmatrix} \tilde{\gamma} \\ \tilde{Z}^0 \\ \cdots \end{pmatrix} = \begin{pmatrix} c_W & s_W \cdots \\ -s_W & c_W \cdots \\ \cdots & \cdots \end{pmatrix}\begin{pmatrix} \tilde{B} \\ \tilde{W} \\ \cdots \end{pmatrix} = A_W\begin{pmatrix} \tilde{B} \\ \tilde{W} \\ \cdots \end{pmatrix},$$

(15)

where the dots indicate that all other states are just multiplied by the unit matrix. Thus when dealing with this new basis $(\tilde{\gamma}, \tilde{Z}^0, \tilde{H}_u, \tilde{H}_d, \nu_e, \nu_\mu, \nu_\tau)$, the mixing matrix is

$$\mathcal{N}' = \mathcal{N} A_W^T,$$

(16)

where only the first two states are rotated.

IV. GRAVITINO DECAY

Indirect observation of the gravitino becomes a possibility due to its decay to ordinary particles. In this section

we calculate the possible decay channels of the gravitino as a dark matter candidate, assuming that $m_{3/2} < m_W$. We then relate these results to experimental bounds on the decay products and on the RPV parameters.

A. Two-body decay

When R-parity is conserved the gravitino can radiatively decay into a photon via the following term in the Lagrangian:

$$\mathcal{L} \ni -\frac{1}{4M_P} \bar{\psi}_\mu \sigma^{\nu\rho} \gamma^\mu \lambda_\gamma F_{\nu\rho}, \tag{17}$$

where M_P is the Planck mass, ψ_μ is the spin-3/2 gravitino field, λ_γ is the spin-1/2 photino field, $F_{\nu\rho} = \partial_\nu A_\rho - \partial_\rho A_\nu$ is the photon field strength, and A_μ is the photon field. This coupling might in principle be modified by a factor of order 1. In this work however we assume that (17) is the exact form of the coupling. Variations of the final result can then be studied by order-1 shifts of the Planck mass M_P. This Lagrangian term induces the following decay:
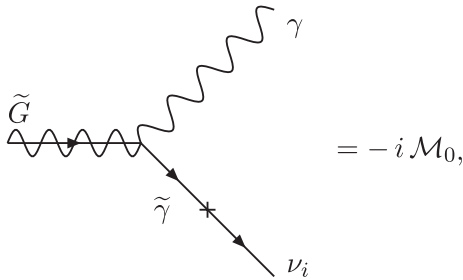
where the cross indicates that we are picking the photino component of the corresponding neutrino, which mix due to violation of R-parity. The amplitude for this decay is

$$\mathcal{M}_0 = -\frac{i}{4M_P}\{\bar{\nu}(q,s)\gamma^\mu[\not{k},\gamma^\nu]\psi_\mu(p,\lambda)\}\epsilon_\mu(k,m)U_{\tilde{\gamma}\nu}, \tag{18}$$

where $U_{\tilde{\gamma}\nu}$ is the amount of photino in the neutrino fields, as indicated by the neutrino eigenvector. We write the gravitino field as the tensor product of a spin-1/2 field with a spin-1 field,

$$\psi_\mu(p,\lambda) = \sum_{s,m}\langle 1/2, s; 1, m | 3/2, \lambda\rangle u(p,s)\epsilon_\mu(p,m), \tag{19}$$

obtaining the following completeness relation [11]:

$$\sum_\lambda \psi_\mu(p,\lambda)\bar{\psi}_\nu(p,\lambda)$$
$$= -(\not{p} - m_{3/2})\left[\left(g_{\mu\nu} - \frac{p_\mu p_\nu}{m_{3/2}^2}\right)\right.$$
$$\left. - \frac{1}{3}\left(g_{\mu\sigma} - \frac{p_\mu p_\sigma}{m_{3/2}^2}\right)\left(g_{\nu\lambda} - \frac{p_\nu p_\lambda}{m_{3/2}^2}\right)\gamma^\sigma\gamma^\lambda\right]. \tag{20}$$

Knowing the above relation, the calculation of the differential cross section is standard, giving the result

$$\frac{d\Gamma}{dE_\gamma d\Omega} = \frac{\langle|\mathcal{M}_0|^2\rangle}{64\pi^2 m_{3/2}}\delta\left(E_\gamma - \frac{m_{3/2}}{2}\right)$$
$$= \frac{m_{3/2}^3}{128\pi^2 M_P^2}|U_{\tilde{\gamma}\nu}|^2\delta\left(E_\gamma - \frac{m_{3/2}}{2}\right), \tag{21}$$

which is independent of the angles as expected. The total decay rate is then

$$\Gamma(\tilde{G} \to \gamma\nu) = \frac{m_{3/2}^3}{32\pi M_P^2}|U_{\tilde{\gamma}\nu}|^2. \tag{22}$$

For a gravitino mass $m_{3/2} < m_W$ this is the only kinematically allowed two-body decay. By using the relation in Eq. (16) one finds that the photino-neutrino mixing factor in PSS is

$$U_{\tilde{\gamma}\nu_i} = \mathcal{N}_{i1}c_W + \mathcal{N}_{i2}s_W, \tag{23}$$

with $i = 5, 6, 7$ labeling the neutrino generation, and where $t_W = g'/g$ is the tangent of the weak mixing angle. Using Eqs. (8)–(10), we find

$$U_{\tilde{\gamma}\nu_i} \simeq \frac{\mu}{2(\det M_{\chi^0})}(\tilde{g}_d M_1 s_W - \tilde{g}'_d M_2 c_W)\Lambda_i. \tag{24}$$

For the numerical calculations we will require the sum over the generations of the square of the mixing factor,

$$|U_{\tilde{\gamma}\nu}|^2 := \sum_i U_{\tilde{\gamma}\nu_i}^2$$
$$\simeq \frac{\mu^2}{4(\det M_{\chi^0})^2}(\tilde{g}_d M_1 s_W - \tilde{g}'_d M_2 c_W)^2|\vec{\Lambda}|^2. \tag{25}$$

This is because we do not distinguish the different neutrino flavors.

B. Three-body decays

When studying the three-body decay, a more general part of the interaction Lagrangian comes into play,

$$\mathcal{L} \ni -\frac{i}{\sqrt{2}M_P}[(D_\mu^* \phi^{i*})\bar{\psi}_\nu \gamma^\mu \gamma^\nu P_L \chi^i$$
$$- (D_\mu \phi^i)\bar{\chi}^i P_R \gamma^\nu \gamma^\mu \psi_\nu]$$
$$- \frac{i}{8M_P}\bar{\psi}_\mu[\gamma^\nu,\gamma^\rho]\gamma^\mu \lambda^{(\alpha)a}F_{\nu\rho}^{(\alpha)a}, \tag{26}$$

where the second line is in analogy to (17) and the first line introduces additional couplings with scalar fields ϕ. The three-body decays of the gravitino were studied in detail for the first time in [20,21], where explicit formulas are given. Nevertheless, our calculations have yielded that the three-body results in [20] have to be corrected. We agree, however, with the conclusion that the three-body decays

are indeed important, and cannot be neglected. We find three-body decay branching ratios of the order of 10% for gravitino masses of order 10 GeV, and greater for larger masses. The exact formulas for the amplitudes of the contributing diagrams are given in the Appendix.

First we consider the gravitino decay into a fermion pair and a neutrino. The first pair of diagrams is three-body decays via an intermediate photon and Z boson,
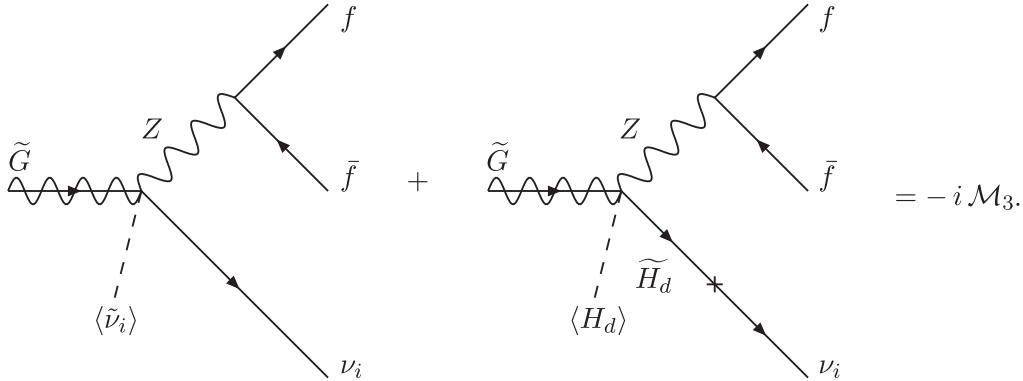

$$= -i\mathcal{M}_{1,2},$$
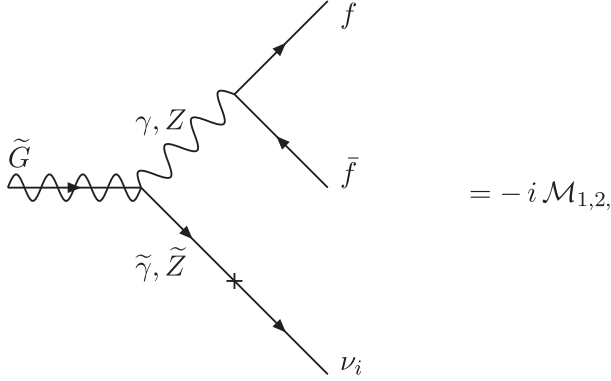
where the cross means we take the photino (or zino) component in the neutrino field. These two amplitudes are equal to

$$= -i\mathcal{M}_3.$$

The first amplitude is proportional to $b_i v_u$ and the second to $v_d(\epsilon_i/\mu)$, in such a way that the combined amplitude $\mathcal{M}_3$ is proportional to Λ_i,

$$
\begin{aligned}
\mathcal{M}_3 = i\frac{-i}{(k^2 - m_Z^2) + im_Z\Gamma_Z}\bar{u}(k_1) \\
\times \frac{-ig}{c_W}\gamma_\mu(c_V^f + c_A^f\gamma_5)v(k_2)\bar{u}(q) \\
\times \frac{-ig\Lambda_i}{4c_W\mu M_P}P_R\gamma^\alpha\gamma^\mu\psi_\alpha(p),
\end{aligned}
\tag{29}
$$

whose contribution to the decay rate is also given in the Appendix. Since the neutrino is not directly detected, a sum over flavors must be done [as in Eq. (25)], after which it is clear that the decay rate will satisfy $\Gamma(\tilde{G} \to f\bar{f}\nu) \propto |\vec{\Lambda}|^2$.

$$
\begin{aligned}
\mathcal{M}_1 = i\frac{-i}{k^2}\bar{u}(k_1)(-iq_f)\gamma_\mu v(k_2)\bar{u}(q) \\
\times \frac{-iU_{\tilde{\gamma}\nu}}{4M_P}\gamma^\alpha(k\!\!\!/\gamma^\mu - \gamma^\mu k\!\!\!/)\psi_\alpha(p),
\end{aligned}
$$

$$
\begin{aligned}
\mathcal{M}_2 = i\frac{-i}{(k^2 - m_Z^2) + im_Z\Gamma_Z}\bar{u}(k_1) \\
\times \frac{-ig}{c_W}\gamma_\mu(c_V^f + c_A^f\gamma_5)v(k_2)\bar{u}(q) \\
\times \frac{-iU_{\tilde{Z}\nu}}{4M_P}\gamma^\alpha(k\!\!\!/\gamma^\mu - \gamma^\mu k\!\!\!/)\psi_\alpha(p),
\end{aligned}
\tag{27}
$$

with $c_V^f = T_3^f/2 - q_f s_W^2$ and $c_A^f = -T_3^f/2$. Their contribution to the decay rate is given in the Appendix. The photino-neutrino mixing is given in Eq. (24), while an analogous calculation for the zino-neutrino mixing gives

$$
U_{\tilde{Z}\nu_i} \simeq -\frac{\mu}{2(\det M_{\chi^0})}(\tilde{g}_d M_1 c_W + \tilde{g}_d' M_2 s_W)\Lambda_i. \tag{28}
$$

To the previous two amplitudes we add a contribution coming from quartic couplings between the gravitino, a gauge boson, and a scalar with its fermionic partner, with the scalar acquiring a vacuum expectation value,
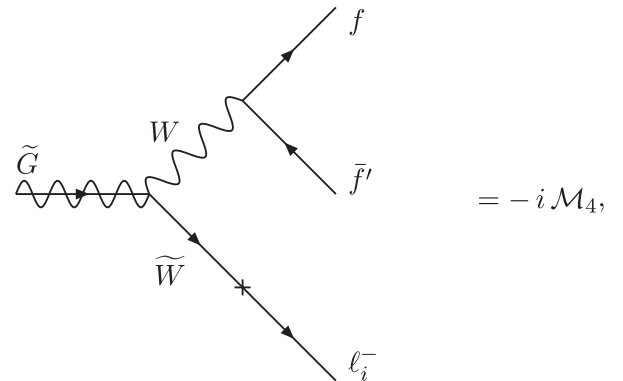
Now we consider the gravitino decay into two fermions and a charged lepton. The decay via a W gauge boson is represented by the Feynman diagram


$$= -i\mathcal{M}_4,$$

whose amplitude can be shown to be

$$\mathcal{M}_4 = i \frac{-i}{(k^2 - m_W^2) + im_W \Gamma_W} \bar{u}(k_1)$$

$$\times \frac{-ig}{2\sqrt{2}} \gamma_\mu (1 - \gamma_5) v(k_2) \bar{u}(q)$$

$$\times \frac{-iU_{\tilde{W}\ell}}{4M_P} \gamma^\alpha (\not{k}\gamma^\mu - \gamma^\mu \not{k}) \psi_\alpha(p).$$

Its contribution to the decay rate is given in the Appendix, and it is proportional to the wino mixing to charged leptons, given by

$$U_{\tilde{W}\ell_i} \simeq -\frac{\tilde{g}_d}{\sqrt{2}(\det M_{\chi^+})} \Lambda_i, \tag{30}$$

where M_{χ^+} is the chargino mass matrix [7]. This graph is complemented by an amplitude coming from quartic couplings between the gravitino, a W gauge boson, and a neutral scalar with its charged fermionic partner, with the scalar acquiring a vacuum expectation value,

$$= -i\mathcal{M}_5.$$
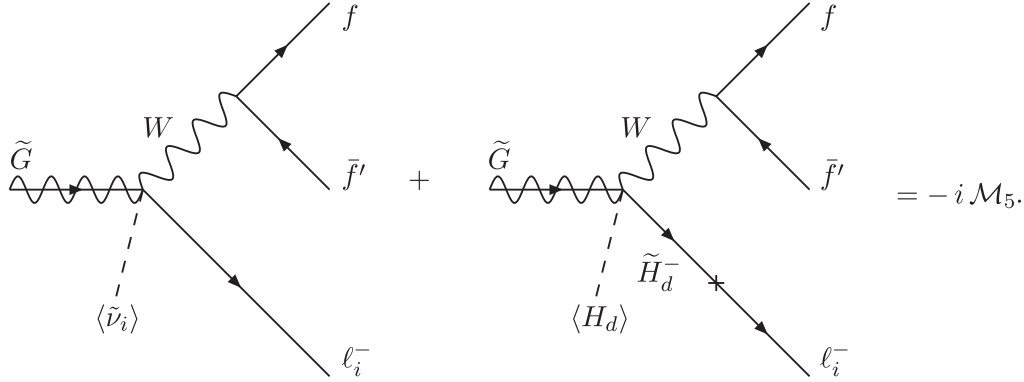
As before, the first amplitude is proportional to $b_i v_u$ and the second to $v_d(\epsilon_i/\mu)$, such that the combined amplitude $\mathcal{M}_5$ is proportional to Λ_i,

$$\mathcal{M}_5 = i \frac{-i}{(k^2 - m_W^2) + im_W \Gamma_W} \bar{u}(k_1)$$

$$\times \frac{-ig}{2\sqrt{2}} \gamma_\mu (1 - \gamma_5) v(k_2) \bar{u}(q)$$

$$\times \frac{-ig\Lambda_i}{2\sqrt{2}\mu M_P} P_R \gamma^\alpha \gamma^\mu \psi_\alpha(p). \tag{31}$$

Its contribution to the decay rate is also given in the Appendix. Note that when fermion f is a charged lepton and f' is a neutrino, we get interference between diagrams $\mathcal{M}_{1,2,3}$ on one hand and $\mathcal{M}_{4,5}$ on the other. This is because the decay $\tilde{G} \to \ell_i^+ \ell_i^- \nu_j$ can proceed via a Z or a W gauge boson. In addition, note that $\Gamma(\tilde{G} \to f\bar{f}'\ell_i^-) = \Gamma(\tilde{G} \to f'\bar{f}\ell_i^+)$, thus we multiply the first one by 2.

The decay rate for the three-body decays of a gravitino can be written as a sum of the various terms given in the Appendix. We sum over three generations, and neglect the masses of the final states. The end result is proportional to $|\vec{\Lambda}|^2$. Thus, in the branching ratio the factor $|\vec{\Lambda}|^2$ cancels, depending only on M_1, M_2, and the gravitino mass $m_{3/2}$ [20]. Here we work with the assumption $M_2 \simeq 2M_1$. The result is shown in Fig. 1, where we plot the branching ratio as a function of $m_{3/2}$ for the three values of $M_1 = 100, 300,$ and 500 GeV. One observes that the three-body decay becomes important for large gravitino masses $m_{3/2}$ and large M_1. The dependency on $m_{3/2}$ can be understood as

a phase-space effect in the three-body decay rate. The influence of M_1 on the branching ratio can be understood by the fact that the two-body and three-body decays, by the virtue of the mixings $U_{\tilde{\gamma}\nu}$ and $U_{\tilde{Z}\nu}$, respectively, get suppressed by growing M_1. In contrast the parts of the three-body decays that contain vacuum expectation values $\langle \tilde{\nu}_i \rangle$ and $\langle H_d \rangle$ do not experience this suppression and thus become more important in the regime of large M_1. Those effects are also present in [20], it is only the form of the
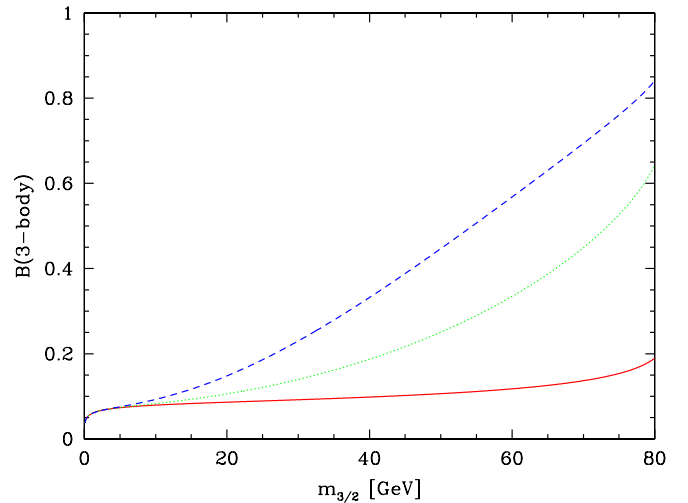

FIG. 1 (color online). Branching ratio of the three-body decay of the gravitino as a function of its mass $m_{3/2}$, red solid line for $M_1 = 100$ GeV, green dotted line for $M_1 = 300$ GeV, and blue dashed line for $M_1 = 500$ GeV.

curves that turned out to change in the corrected version. For the masses we are interested in here, $m_{3/2} \lesssim 10$ GeV, the three-body decay is $\lesssim 10\%$ and with small dependence on the gaugino mass. For larger gravitino masses the branching ratio can be as large as 80%. Since the calculations are being carried out in the Feynman gauge, there are in principle also diagrams containing Goldstone bosons in the propagator. However, due to the coupling of the Goldstone bosons, those contributions vanish in the limit of light fermion masses.

C. Induced photon flux

The photon spectrum produced by the decay of the gravitino consists of a monoenergetic line of energy $m_{3/2}/2$ from the two-body decay, plus a continuum distribution from the three-body decays. The exact form of the spectrum, which depends on $m_{3/2}$ and M_1, was studied in detail in [20,21] using an event generator. Here we are interested in obtaining constraints on the gravitino parameters, for which it suffices as an approximation to consider only the photon line from the two-body decay, as this is the most prominent feature of the spectrum for values of M_1 up to 1 TeV [20]. Including the three-body decay would make our final conclusions slightly more stringent.

The observed spectrum is calculated from the flux of gamma rays expected at Earth. This flux is the sum of two contributions, one from the gravitinos decaying in the galactic halo, and one from the gravitinos decaying at cosmological distances. It has been shown that the first contribution is highly dominant, and so we will neglect the second one [18]. In this way the differential flux, as a function of the photon energy E, has the following simple form [18,19]:

$$E^2 \frac{dJ_{\text{halo}}}{dE} = \frac{D_\gamma m_{3/2}}{2} \delta\left(E - \frac{m_{3/2}}{2}\right), \qquad (32)$$

with

$$D_\gamma = \frac{\Gamma(\tilde{G} \to \gamma \nu)}{8\pi} \left\langle \int_{\text{LOS}} \rho_{\text{halo}}(\vec{r}) d\ell \right\rangle = d_\gamma \Gamma(\tilde{G} \to \gamma \nu). \qquad (33)$$

The constant d_γ depends on the dark matter density profile of the halo, and on the region of the sky considered for averaging the flux (denoted by the term in brackets above, where LOS means line of sight). Using the Navarro-Frenk-White profile [38], and considering the region $|b| \geq 10°$ for the average (with b denoting the latitude in galactic coordinates), we find

$$d_\gamma = 0.80 \times 10^{24} [\text{MeV cm}^{-2} \text{ str}^{-1}]. \qquad (34)$$

This region of the sky was the one considered by the Fermi LAT Collaboration in the derivation of the extragalactic diffuse spectrum [23].

V. LIMITS AND CONSTRAINTS

A. Constraint from the observed photon spectrum

The fact that the line produced by the gravitino two-body decay has not been observed gives constraints on the mass and the lifetime of the gravitino. Assuming that the extragalactic diffuse spectrum measured by Fermi LAT can be correctly modeled in terms of known sources [22], one can use this spectrum to find constraints [23,39].

After the convolution between the calculated flux in Eq. (32) and a Gaussian distribution, we find

$$E^2 \frac{dJ_{\text{halo}}}{dE} = \frac{D_\gamma m_{3/2}}{2} \frac{1}{\sqrt{2\pi\sigma^2}} e^{-(E-m_{3/2}/2)^2/2\sigma^2}, \qquad (35)$$

where σ is related to the energy-dependent resolution of the Fermi LAT instrument p evaluated at the two-body peak

$$\sigma = pE = p\frac{m_{3/2}}{2}. \qquad (36)$$

The energy dependence of p evaluated at $E = m_{3/2}/2$ can be approximated by [24,40]

$$p(m_{3/2}) = 0.349 - 0.142 \log\left(\frac{m_{3/2}}{2 \text{ MeV}}\right)$$
$$+ 0.019 \log^2\left(\frac{m_{3/2}}{2 \text{ MeV}}\right). \qquad (37)$$

Thus, the maximum of the photon spectrum is given by

$$\left(E^2 \frac{dJ_{\text{halo}}}{dE}\right)_{\text{max}} = \frac{D_\gamma}{p(m_{3/2})\sqrt{2\pi}}. \qquad (38)$$

On the other hand, the intensity or the integrated flux for the extragalactic diffuse emission (for the range $E > 100$ MeV and the sky region $|b| \geq 10°$) was measured by the Fermi LAT Collaboration [23],

$$I(>100 \text{ MeV}) = \int_{100}^\infty \frac{dJ}{dE}$$
$$= (1.03 \pm 0.17) \times 10^{-5} [\text{cm}^{-2} \text{ s}^{-1} \text{ str}^{-1}], \qquad (39)$$

together with the observation that the spectrum can be fitted by a power law $dJ/dE \propto E^{-\gamma}$, with index $\gamma = 2.41 \pm 0.05$. From this we calculate the spectrum to be

$$E^2 \frac{dJ}{dE} = (9.6 \pm 1.6) \times 10^{-3} [\text{MeV cm}^{-2} \text{ s}^{-1} \text{ str}^{-1}]$$
$$\times \left(\frac{E}{1 \text{ MeV}}\right)^{2-\gamma}, \qquad (40)$$

where the error was directly calculated from the error in the integrated flux using Eq. (39).

As we mentioned before, we assume that the central value of the spectrum can be explained by models of known sources [22]. We impose that the extra contribution from the gravitino source is smaller than a 3σ error margin.

This gravitino contribution is related to the decay rate $\Gamma(\tilde{G} \to \gamma\nu)$ through Eqs. (33) and (38). By introducing the total decay width, $\tau_{3/2}^{-1} = \Gamma(\tilde{G} \to \gamma\nu) + \Gamma(\text{3-body})$, we find the following restriction on the gravitino lifetime:

$$\left(\frac{\tau_{3/2}}{10^{27} \text{ s}}\right) > \frac{0.851}{p(m_{3/2})} B(\tilde{G} \to \gamma\nu)\left(\frac{m_{3/2}}{1 \text{ GeV}}\right)^{\gamma-2}, \quad (41)$$

where $B(\tilde{G} \to \gamma\nu)$ denotes the branching ratio of the two-body decay. In this way Eq. (41) defines a region in the $m_{3/2} - \tau_{3/2}$ plane consistent with the nonobservation of the gravitino decay by Fermi LAT.

The gravitino two-body decay width $\Gamma(\tilde{G} \to \gamma\nu)$ is given in Eq. (22). If we sum over all neutrino species it becomes proportional to $|\vec{\Lambda}|^2$, via $|U_{\tilde{\gamma}\nu}|^2$ in Eq. (25). The three-body decay width is also proportional to $|\vec{\Lambda}|^2$. The reasons are analogous to the two-body decay, since after summing over lepton generations we see that $|\mathcal{M}_1|^2$ is proportional to $|U_{\tilde{\gamma}\nu}|^2$, $|\mathcal{M}_2|^2$ is proportional to $|U_{\tilde{Z}\nu}|^2$ [Eq. (28)], and $|\mathcal{M}_4|^2$ is proportional to $|U_{\tilde{W}\ell}|^2$ [Eq. (30)]. In addition, amplitudes $|\mathcal{M}_3|^2$ and $|\mathcal{M}_5|^2$ are directly proportional to $|\vec{\Lambda}|^2$ as can be seen from Eqs. (29) and (31). In this way, the gravitino lifetime becomes large for two reasons, because the Planck mass is large and because BRPV is small: $\tau_{3/2}^{-1} \propto |\vec{\Lambda}|^2/M_P^2$.

We display experimental constraints on the model in the $m_{3/2}$-$\tau_{3/2}$ plane, with the first one given by Eq. (41). This constraint depends also on $|U_{\tilde{\gamma}\nu}|^2$ and the gaugino masses. In fact, the whole decay rate $\Gamma(\text{three-body})$ can be factored out by $|U_{\tilde{\gamma}\nu}|^2$ with the remaining factors depending on M_1 and M_2, but with the dependence on μ being in first approximation negligible. We further use the simplifying assumption $M_2 = 2M_1$ motivated by minimal supergravity models. In this way, we display the constraints in the plane $m_{3/2}$-$\tau_{3/2}$ as a function of $|U_{\tilde{\gamma}\nu}|^2$ and M_1. In the first constraint in Eq. (41) though, the dependence on $|U_{\tilde{\gamma}\nu}|$ drops out.

B. Constraints from the neutrino mass matrix

Further constraints appear from neutrino physics, controlled by the BRPV parameters Λ_i and ϵ_i, and by MSSM parameters like gaugino and Higgsino masses. We do a scan over parameter space looking for good solutions to neutrino observables. The range in which we vary the parameters is given in Table I. We define a χ^2 value for each point in parameter space as follows:

$$\chi^2 = \left(\frac{10^3 \Delta m_{\text{atm}}^2 - 2.4}{0.4}\right)^2 + \left(\frac{10^5 \Delta m_{\text{sol}}^2 - 7.7}{0.6}\right)^2$$
$$+ \left(\frac{\sin^2\theta_{\text{atm}} - 0.505}{0.165}\right)^2 + \left(\frac{\sin^2\theta_{\text{sol}} - 0.33}{0.07}\right)^2, \quad (42)$$

allowing a 3σ deviation [41]. The point is accepted if $\chi^2 < 4$, plus the additional condition that the reactor angle

TABLE I.   Scanned ranges for PSS and RPV parameters.

Supersymmetry parameter	Scanned range	Units
$\tan\beta$	[2, 50]	
$|\mu|$	[0, 1000]	GeV
M_2	$2M_1$	GeV
M_1	100, 300, 500	GeV
m_h	[114, 140]	GeV
m_A	[50, 6000]	GeV
Q	951.7	
RPV parameter		
ϵ_1	[−1, 1]	GeV
ϵ_2	[−1, 1]	GeV
ϵ_3	[−1, 1]	GeV
Λ_1	[−1, 1]	GeV^2
Λ_2	[−1, 1]	GeV^2
Λ_3	[−1, 1]	GeV^2

satisfies the bound $\sin^2\theta_{\text{reac}} < 0.05$. Since $\tau_{3/2}$ depends directly on $|U_{\tilde{\gamma}\nu}|$ we determined its maximal and minimal values for a given M_1 compatible with neutrino physics. The numerical results are given in Table II. One sees that the range of possible values for $|U_{\tilde{\gamma}\nu}|^2$ depends on the value of M_1, with the maximal value being around 3 orders of magnitude greater than the minimum value for each case. Since the gravitino lifetime $\tau_{3/2}^{-1} = \Gamma(\tilde{G} \to \gamma\nu) + \Gamma(\text{three-body})$ depends on $|U_{\tilde{\gamma}\nu}|^2$, $m_{3/2}$, and M_1, this imposes two extra constraints in the $m_{3/2}$-$\tau_{3/2}$ plane that complement the one in Eq. (41).

VI. COMBINED CONSTRAINTS AND RESULTS

The combination of the constraints found in the previous section defines an allowed region in the $m_{3/2}$-$\tau_{3/2}$ plane. This region is shown in Figs. 2(a) and 2(b) for the gaugino mass, $M_1 = 100$, and 500 GeV. One sees that the constraint from the photon spectrum, when taken together with the maximal value of $|U_{\tilde{\gamma}\nu}|^2$ consistent with neutrino experiments, gives a lower bound on the gravitino lifetime. In all cases that we studied, this bound is several orders of magnitude larger than the age of the Universe, compatible with a good candidate for dark matter. Even more interestingly, we see from Fig. 2 that the constraint from the photon spectrum, when combined with the minimum

TABLE II.   Maximal and minimal values of $|U_{\tilde{\gamma}\nu}|^2$, consistent with neutrino experiments, for three different values of M_1.

M_1	$|U_{\tilde{\gamma}\nu}|^2$ (min)	$|U_{\tilde{\gamma}\nu}|^2$ (max)
100 GeV	2×10^{-16}	4×10^{-13}
300 GeV	2×10^{-17}	3×10^{-14}
500 GeV	1×10^{-17}	1×10^{-14}

(a) *Allowed region for $M_1 = 100$ GeV.*
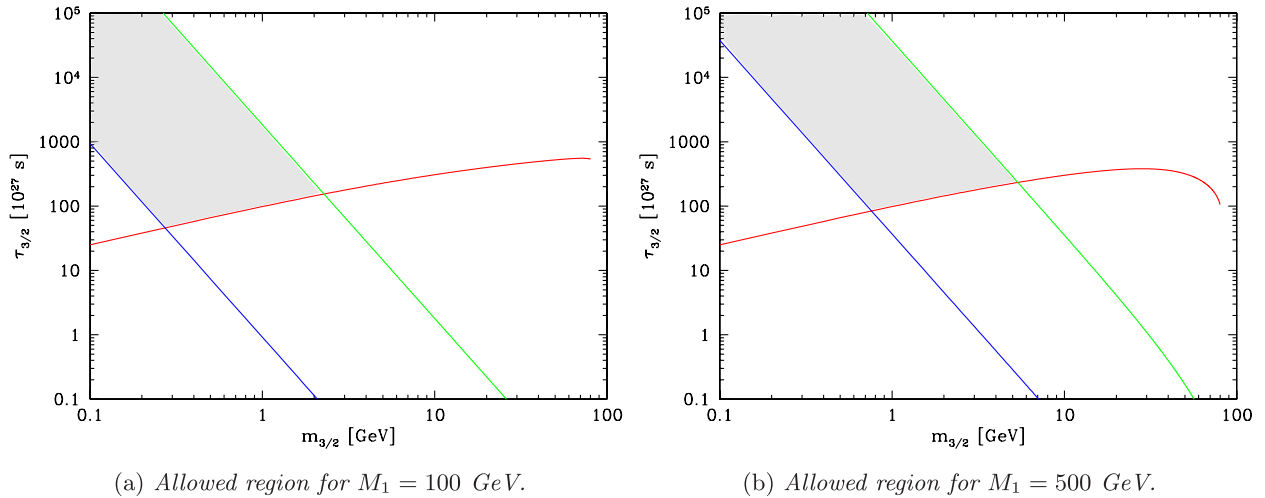

(b) *Allowed region for $M_1 = 500$ GeV.*

FIG. 2 (color online). Allowed (shaded) region in the $m_{3/2}$-$\tau_{3/2}$ plane. The region above the nearly horizontal red line is allowed by the constraint in Eq. (41). The region between the oblique lines is allowed by minimum green and maximum blue values of $|U_{\tilde{\gamma}\nu}|^2$.

allowed value of $|U_{\tilde{\gamma}\nu}|^2$, imposes an upper bound on the gravitino mass. This bound is near 2, 4, and 5 GeV for $M_1 = 100$, 300, and 500 GeV.

We also note from these graphs how the three-body decays of the gravitino become more important as M_1 increases. In particular, the constraint coming from the photon spectrum analysis becomes less stringent as the gravitino mass gets closer to m_W, which is quite evident for the case of $M_1 = 500$ GeV. This is expected from the fact that the strength of the gravitino photon line is proportional to the branching ratio of the two-body decay. Conversely, for a gravitino of mass below ~ 10 GeV, this branching ratio is close to 1, and so from Eq. (22) we see that the lifetime is approximately proportional to $m_{3/2}^{-3}$, as can be noted in Fig. 2.

We stress that this analysis assumes that $m_{3/2} < m_W$. For a gravitino with a mass greater than the Z boson mass the two-body decays $\tilde{G} \to Z\nu$ and $\tilde{G} \to W\ell$ will be kinematically allowed. As shown in Ref. [15], the branching ratio of the decay $\tilde{G} \to \gamma\nu$ becomes very small for a gravitino mass above 100 GeV, and so the monochromatic line in the photon spectrum becomes less important. A more detailed analysis of the photon spectrum produced by the decay of the gravitino would be required in that case, which would need to include the fragmentation of the W and Z bosons in addition to the contribution from the three-body decays.

VII. SUMMARY

It is explained how PSS in combination with RPV allows one to generate the neutrino masses and mixings at the one-loop level. Then it is investigated whether in this model the gravitino still is a good dark matter candidate. In order to do this the gravitino decay rates into two- and three-body states are calculated. In the three-body decay corrections

are found to previous calculations. Since for relatively small gravitino masses the decay is dominated by the two-body decay, the corrections in the three-body case do not affect the final result. Those rates allow one to calculate the additional photon flux that is induced by the gravitino decay. Comparison of this photon flux with recent data from the Fermi LAT Collaboration, allows restrictions on our model in the gravitino decay process.

Finally, combining the restrictions obtained in the neutrino sector with the restrictions in the gravitino dark matter sector of the same model, an upper limit on the gravitino mass $m_{3/2} < 6$ GeV is found. The exact values of the maximal $m_{3/2}$ and the minimal $\tau_{3/2}$ in our model are given in Table III. One observes a relatively weak M_1 dependence.

It is interesting to note that most direct dark matter search experiments disfavor the typical heavy dark matter particle that appears in R-parity conserving supersymmetric models [27,28]. The bound, however, is not nearly as tight for a light dark matter gravitino as it is found here. On the other hand, with the derived limit, the model turns out to be directly testable. For instance, if a relatively heavy dark matter particle is found with $m_{3/2} \gg 10$ GeV, one could immediately conclude that this model is ruled out. This feature of testability and the possibility of falsification can be seen as a strong advantage over many other models.

TABLE III. Minimal values of $\tau_{3/2}$ and maximal values of $m_{3/2}$ as a function of M_1.

M_1 [GeV]	$\tau_{3/2}$ (min) [s]	$m_{3/2}$ (max) [GeV]
100	4.7×10^{28}	2.3
300	7.2×10^{28}	4.4
500	8.6×10^{28}	5.3

ACKNOWLEDGMENTS

APPENDIX A: THREE-BODY DECAY FORMULAS

We label the five relevant diagrams with indices 1 to 5 as indicated in the text. For the photon and Z-mediated diagrams we define the invariant masses $s := (k_1 + k_2)^2$, and $t := (k_1 + q)^2$, where k_1, k_2, and q are the 4-momenta of the fermion, antifermion, and neutrino, respectively. For the spin-averaged squared amplitudes and interferences we find (we define $m \equiv m_{3/2}$ for simplicity)

$$\langle|\mathcal{M}_1|^2\rangle = \frac{1}{4}\left(\frac{q_f^2|U_{\tilde{\gamma}\nu_i}|^2}{16M_P^2}\right)\frac{1}{s^2}T_{11}, \tag{A1}$$

$$\langle|\mathcal{M}_2|^2\rangle = \frac{1}{4}\left(\frac{g^2|U_{\tilde{Z}\nu_i}|^2}{16c_W^2M_P^2}\right)\frac{1}{(s - m_Z^2)^2 + m_Z^2\Gamma_Z^2}T_{22}, \tag{A2}$$

$$\langle|\mathcal{M}_3|^2\rangle = \frac{1}{4}\left(\frac{g^4\Lambda_i^2}{64\mu^2c_W^4M_P^2}\right)\frac{1}{(s - m_Z^2)^2 + m_Z^2\Gamma_Z^2}T_{33}, \tag{A3}$$

$$2\Re\langle\mathcal{M}_1^*\mathcal{M}_2\rangle = \frac{2}{4}\left(\frac{gq_fU_{\tilde{\gamma}\nu_i}U_{\tilde{Z}\nu_i}}{16c_WM_P^2}\right)$$
$$\times \frac{(s - m_Z^2)}{s[(s - m_Z^2)^2 + m_Z^2\Gamma_Z^2]}T_{12}, \tag{A4}$$

$$2\Re\langle\mathcal{M}_1^*\mathcal{M}_3\rangle = \frac{2}{4}\left(\frac{g^2q_fU_{\tilde{\gamma}\nu_i}\Lambda_i}{32\mu c_W^2M_P^2}\right)$$
$$\times \frac{(s - m_Z^2)}{s[(s - m_Z^2)^2 + m_Z^2\Gamma_Z^2]}T_{13}, \tag{A5}$$

$$2\Re\langle\mathcal{M}_2^*\mathcal{M}_3\rangle = \frac{2}{4}\left(\frac{g^3U_{\tilde{Z}\nu_i}\Lambda_i}{32\mu c_W^3M_P^2}\right)\frac{1}{(s - m_Z^2)^2 + m_Z^2\Gamma_Z^2}T_{23}. \tag{A6}$$

For the W-mediated diagrams, we define s and t as above, with k_1, k_2, and q the 4-momenta of the neutrino, antilepton, and lepton, respectively. We find

$$\langle|\mathcal{M}_4|^2\rangle = \frac{1}{4}\left(\frac{g^2|U_{\tilde{W}\ell_i'}|^2}{128M_P^2}\right)\frac{1}{(s - m_W^2)^2 + m_W^2\Gamma_W^2}T_{44}, \tag{A7}$$

$$\langle|\mathcal{M}_5|^2\rangle = \frac{1}{4}\left(\frac{g^4\Lambda_i^2}{256\mu^2M_P^2}\right)\frac{1}{(s - m_W^2)^2 + m_W^2\Gamma_W^2}T_{55}, \tag{A8}$$

$$2\Re\langle\mathcal{M}_4^*\mathcal{M}_5\rangle = \frac{2}{4}\left(\frac{g^3U_{\tilde{W}\ell_i'}\Lambda_i}{128\sqrt{2}\mu M_P^2}\right)$$
$$\times \frac{1}{(s - m_W^2)^2 + m_W^2\Gamma_W^2}T_{45}. \tag{A9}$$

Finally, for the interference terms between these two groups of diagrams (when $f = \ell' = \ell$), we define s and t as above, with k_1, k_2, and q the 4-momenta of the lepton, antilepton, and neutrino, respectively. We find

$$2\Re\langle\mathcal{M}_1^*\mathcal{M}_4\rangle = \frac{2}{4}\left(\frac{gq_fU_{\tilde{\gamma}\nu_i}U_{\tilde{W}\ell_i}}{32\sqrt{2}M_P^2}\right)\frac{(m^2 - (s + t) - m_W^2)}{s[(m^2 - (s + t) - m_W^2)^2 + m_W^2\Gamma_W^2]}T_{14}, \tag{A10}$$

$$2\Re\langle\mathcal{M}_2^*\mathcal{M}_4\rangle = \frac{2}{4}\left(\frac{g^2U_{\tilde{Z}\nu_i}U_{\tilde{W}\ell_i}}{32\sqrt{2}c_WM_P^2}\right)\frac{(s - m_Z^2)(m^2 - (s + t) - m_W^2) + m_Zm_W\Gamma_Z\Gamma_W}{[(s - m_Z^2)^2 + m_Z^2\Gamma_Z^2][(m^2 - (s + t) - m_W^2)^2 + m_W^2\Gamma_W^2]}T_{24}, \tag{A11}$$

$$2\Re\langle\mathcal{M}_3^*\mathcal{M}_4\rangle = \frac{2}{4}\left(\frac{g^3U_{\tilde{W}\ell_i}\Lambda_i}{64\sqrt{2}\mu c_W^2M_P^2}\right)\frac{(s - m_Z^2)(m^2 - (s + t) - m_W^2) + m_Zm_W\Gamma_Z\Gamma_W}{[(s - m_Z^2)^2 + m_Z^2\Gamma_Z^2][(m^2 - (s + t) - m_W^2)^2 + m_W^2\Gamma_W^2]}T_{34}, \tag{A12}$$

$$2\Re\langle\mathcal{M}_1^*\mathcal{M}_5\rangle = \frac{2}{4}\left(\frac{g^2q_fU_{\tilde{\gamma}\nu_i}\Lambda_i}{64\mu M_P^2}\right)\frac{(m^2 - (s + t) - m_W^2)}{s[(m^2 - (s + t) - m_W^2)^2 + m_W^2\Gamma_W^2]}T_{15}, \tag{A13}$$

$$2\Re\langle\mathcal{M}_2^*\mathcal{M}_5\rangle = \frac{2}{4}\left(\frac{g^3U_{\tilde{Z}\nu_i}\Lambda_i}{64\mu c_WM_P^2}\right)\frac{(s - m_Z^2)(m^2 - (s + t) - m_W^2) + m_Zm_W\Gamma_Z\Gamma_W}{[(s - m_Z^2)^2 + m_Z^2\Gamma_Z^2][(m^2 + -(s + t) - m_W^2)^2 + m_W^2\Gamma_W^2]}T_{25}, \tag{A14}$$

$$2\Re\langle\mathcal{M}_3^*\mathcal{M}_5\rangle = \frac{2}{4}\left(\frac{g^4\Lambda_i^2}{128\mu^2c_W^2M_P^2}\right)\frac{(s - m_Z^2)(m^2 - (s + t) - m_W^2) + m_Zm_W\Gamma_Z\Gamma_W}{[(s - m_Z^2)^2 + m_Z^2\Gamma_Z^2][(m^2 - (s + t) - m_W^2)^2 + m_W^2\Gamma_W^2]}T_{35}. \tag{A15}$$

The total amplitude of the three-body decays is given by the sum of all these terms, each being summed over all the relevant flavors and colors of the final states. The traces in Eqs. (A1) to (A15) are given by

$$T_{11} = \frac{64}{3m^2} s\{3m^6 - 3m^4(s + 2t) + m^2(s^2 + 8st + 6t^2) - s(s^2 + 2t(s + t))\}, \tag{A16}$$

$$T_{22} = \frac{64}{3m^2} (c_V^2 + c_A^2) s\{3m^6 - 3m^4(s + 2t) + m^2(s^2 + 6t^2 + 8st) - s(s^2 + 2t(s + t))\}, \tag{A17}$$

$$T_{33} = \frac{64}{3m^2} \{(c_V^2 + c_A^2)(m^2 - s)(m^2(2s + t) - t(s + t)) - 2c_V c_A m^2 s(m^2 - s - 2t)\}, \tag{A18}$$

$$T_{12} = \frac{64}{3m^2} c_V s\{3m^6 - 3m^4(s + 2t) + m^2(s^2 + 8st + 6t^2) - s(s^2 + 2t(s + t))\}, \tag{A19}$$

$$T_{13} = \frac{32}{3m} s\{c_V(3m^4 - 2m^2(s + t) - s^2 + 2st + 2t^2) - c_A(3m^2 - s)(m^2 - s - 2t)\}, \tag{A20}$$

$$T_{23} = \frac{32}{3m} s\{(c_V^2 + c_A^2)(3m^4 - 2m^2(s + t) - s^2 + 2t^2 + 2st) - 2c_V c_A(3m^4 - 2m^2(2s + 3t) + s^2 + 2st)\}, \tag{A21}$$

$$T_{44} = \frac{128}{3m^2} s\{3m^6 - 3m^4(s + 2t) + m^2(s^2 + 8st + 6t^2) - s(s^2 + 2st + 2t^2)\}, \tag{A22}$$

$$T_{55} = \frac{128}{3m^2} \{m^4(3s + t) - m^2(s + t)(3s + t) + st(s + t)\}, \tag{A23}$$

$$T_{45} = \frac{128}{3m} s\{3m^4 - m^2(3s + 4t) + t(2s + t)\}, \tag{A24}$$

$$T_{14} = \frac{64}{3m^2} s\{3m^6 - m^4(3s + 7t) + m^2 t(4s + 5t) - t^2(s + t)\}, \tag{A25}$$

$$T_{24} = \frac{64}{3m^2} (c_V - c_A) s\{3m^6 - m^4(3s + 7t) + m^2 t(4s + 5t) - t^2(s + t)\}, \tag{A26}$$

$$T_{34} = \frac{64}{3m^2} (c_V - c_A)\{m^5(3s + t) - m^3(3s^2 + 6st + 2t^2) + mt(s + t)(2s + t)\}, \tag{A27}$$

$$T_{15} = \frac{64}{3m} s\{3m^4 - m^2(3s + 4t) + t(2s + t)\}, \tag{A28}$$

$$T_{25} = \frac{64}{3m} (c_V - c_A) s\{3m^4 - m^2(3s + 4t) + t(2s + t)\}, \tag{A29}$$

$$T_{35} = \frac{64}{3m^2} (c_V - c_A)\{(m^2 - s)(m^2 s + (m^2 - t)(s + t)) + m^2 s(m^2 - s - 2t)\}. \tag{A30}$$

Finally those amplitudes are applied to the golden rule for decays in order to obtain the partial and total decay rate for each process $\tilde{G} \to 2 + 3 + 4$

$$d\Gamma = |\mathcal{M}|^2 \frac{S}{2m_{3/2}} \left[\frac{d^3 p_2}{(2\pi)^3 2E_2} \frac{d^3 p_3}{(2\pi)^3 2E_3} \frac{d^3 p_4}{(2\pi)^3 2E_4} \right] (2\pi)^4 \delta^4(p_1 - p_2 - p_3 - p_4). \tag{A31}$$

[1] N. Arkani-Hamed and S. Dimopoulos, J. High Energy Phys. 06 (2005) 073; G. F. Giudice and A. Romanino, Nucl. Phys. **B699**, 65 (2004); **B706**, 487(E) (2005).

[2] G. Aad *et al.* (ATLAS Collaboration), arXiv:0901.0512; P. de Jong, AIP Conf. Proc. **1078**, 21 (2009).

[3] R. Barbier *et al.*, Phys. Rep. **420**, 1 (2005).

[4] M. Nowakowski and A. Pilaftsis, Nucl. Phys. **B461**, 19 (1996); R. Hempfling, Nucl. Phys. **B478**, 3 (1996).

[5] M. Hirsch, M. A. Diaz, W. Porod, J. C. Romao, and J. W. F. Valle, Phys. Rev. D **62**, 113008 (2000); **65**, 119901(E) (2002).

[6] E. J. Chun and S. C. Park, J. High Energy Phys. 01 (2005) 009; S. Davidson and M. Losada, Phys. Rev. D **65**, 075025 (2002); J. High Energy Phys. 05 (2000) 021; Y. Grossman and S. Rakshit, Phys. Rev. D **69**, 093002 (2004).

[7] M. A. Diaz, P. Fileviez Perez, and C. Mora, Phys. Rev. D **79**, 013005 (2009).

[8] M. A. Diaz, B. Koch, and B. Panes, Phys. Rev. D **79**, 113009 (2009).

[9] R. Sundrum, J. High Energy Phys. 01 (2011) 062.

[10] M. A. Diaz, F. Garay, and B. Koch, Phys. Rev. D **80**, 113005 (2009).

[11] M. Grefe, Report No. DESY-THESIS-2008-043; L. Covi, arXiv:1003.3819; W. Buchmuller, AIP Conf. Proc. 1200, 155 (2010).

[12] F. Wang, W. Wang, and J. M. Yang, Phys. Rev. D **72**, 077701 (2005).

[13] F. Takayama and M. Yamaguchi, Phys. Lett. B **485**, 388 (2000).

[14] K. Ishiwata, S. Matsumoto, and T. Moroi, Phys. Rev. D **78**, 063505 (2008).

[15] A. Ibarra and D. Tran, Phys. Rev. Lett. **100**, 061301 (2008).

[16] H. Yuksel and M. D. Kistler, Phys. Rev. D **78**, 023502 (2008).

[17] K. Y. Choi, D. E. Lopez-Fogliani, C. Munoz, and R. R. de Austri, J. Cosmol. Astropart. Phys. 03 (2010) 028.

[18] W. Buchmuller, L. Covi, K. Hamaguchi, A. Ibarra, and T. Yanagida, J. High Energy Phys. 03 (2007) 037.

[19] G. Bertone, W. Buchmuller, L. Covi, and A. Ibarra, J. Cosmol. Astropart. Phys. 11 (2007) 003.

[20] K. Y. Choi, D. Restrepo, C. E. Yaguna, and O. Zapata, J. Cosmol. Astropart. Phys. 10 (2010) 033.

[21] K. Y. Choi and C. E. Yaguna, Phys. Rev. D **82**, 015008 (2010).

[22] A. A. Abdo *et al.* (Fermi LAT Collaboration), Astrophys. J. **720**, 435 (2010).

[23] A. A. Abdo *et al.* (Fermi LAT Collaboration), Phys. Rev. Lett. **104**, 101101 (2010).

[24] W. B. Atwood *et al.* (Fermi LAT Collaboration), Astrophys. J. **697**, 1071 (2009).

[25] A. A. Abdo *et al.* (Fermi LAT Collaboration), Phys. Rev. Lett. **103**, 251101 (2009).

[26] A. A. Abdo *et al.* (Fermi LAT Collaboration), Phys. Rev. Lett. **104**, 091302 (2010).

[27] Z. Ahmed *et al.* (CDMS-II Collaboration), Science **327**, 1619 (2010).

[28] E. Aprile *et al.* (XENON100 Collaboration), arXiv:1104.2549.

[29] B. Bajc, T. Enkhbat, D. K. Ghosh, G. Senjanovic, and Y. Zhang, J. High Energy Phys. 05 (2010) 048.

[30] S. L. Chen, R. N. Mohapatra, S. Nussinov, and Y. Zhang, Phys. Lett. B **677**, 311 (2009).

[31] M. Y. Khlopov and A. D. Linde, Phys. Lett. **138B**, 265 (1984).

[32] I. V. Falomkin, G. B. Pontecorvo, M. G. Sapozhnikov, M. Y. Khlopov, F. Balestra, and G. Piragino, Yad. Fiz. **39**, 990 (1984); Nuovo Cimento Soc. Ital. Fis. A **79**, 193 (1984).

[33] M. Y. Khlopov, A. Barrau, and J. Grain, Classical Quantum Gravity **23**, 1875 (2006).

[34] N. Arkani-Hamed, S. Dimopoulos, G. F. Giudice, and A. Romanino, Nucl. Phys. **B709**, 3 (2005).

[35] M. Drees, arXiv:hep-ph/0501106.

[36] B. C. Allanach, A. Dedes, and H. K. Dreiner, Phys. Rev. D **69**, 115002 (2004).

[37] P. Fileviez Perez and S. Spinner, Phys. Rev. D **83**, 035004 (2011).

[38] J. F. Navarro, C. S. Frenk, and S. D. M. White, Astrophys. J. **462**, 563 (1996).

[39] W. Buchmuller, A. Ibarra, T. Shindou, F. Takayama, and D. Tran, J. Cosmol. Astropart. Phys. 09 (2009) 021.

[40] Fermi LAT Collaboration, "Fermi LAT Performance," http://www-glast.slac.stanford.edu/software/IS/glast_lat_performance.htm.

[41] M. Maltoni, T. Schwetz, M. A. Tortola, and J. W. F. Valle, New J. Phys. **6**, 122 (2004).